PERKIN 2

DFT study on the cycloaddition reactions of [*c*]-annelated carbo- and heterocyclic five-membered dienes with ethylene†

Tandapani C. Dinadayalane and G. Narahari Sastry *

Department of Chemistry, Pondicherry University, Pondicherry, 605 014, India

Received (in Cambridge, UK) 12th June 2002, Accepted 10th September 2002
First published as an Advance Article on the web 3rd October 2002

B3LYP/6-31G* calculations were done on a series of [*c*]-annelated heterocyclic five-membered dienes and their cycloaddition transition state structures and products. Cyclobutano[*c*]-, cyclobuteno[*c*]- and benzo[*c*]-fused five-membered rings represent non-aromatic, antiaromatic and aromatic ring fused dienes, respectively, and their reactivity was studied with ethylene as dienophile. In the cases of cyclobutano- and cyclobuteno-fused dienes, the fused portion remains a mere spectator and no significant geometric variations are seen along the reaction coordinate. In contrast, in the benzo-fused systems, the fused benzene ring witnesses significant changes in the bond lengths along the reaction coordinate highlighting the active participation of the π-framework in the reaction. Thus, this may be classified as an [8 + 2] cycloaddition. The benzo[*c*]-fused rings exhibit the lowest activation energies followed by cyclobutano and cyclobuteno analogues, and the exothermicities decrease in the same order. A linear relationship between the reaction exothermicity and activation energy is obtained for the systems under consideration. The percentage bond length alternation on going from reactant to transition state, the Fukui function indices and frontier orbital analysis, extent of charge transfer from diene to dienophile at the transition state, and deformation energies were estimated to explain the reactivity of the dienes with ethylene.

Introduction

Pericyclic reactions represent one of the most important classes of reaction in view of their synthetic potential and have attracted lots of attention both at qualitative and quantitative levels of theory.[1,2] Among them, Diels–Alder reactions are arguably the most important synthetic strategies in accomplishing novel polycyclic organic skeletons, which find applications in various branches of chemistry.[3–8] The long standing controversy over the mechanism has been settled recently and a consensus has emerged.[9] Thus, both concerted and stepwise mechanisms are operative, but in cases of symmetrical diene–dienophile combinations, the stepwise mechanism was found to lie about 2–7 kcal mol^{-1} above the concerted mechanism.[10,11] However, in cases especially where substituents stabilize the radical intermediates, the stepwise mechanism might become more facile in comparison to the concerted one.[10–12]

The Diels–Alder reaction between cyclic five-membered rings and dienophiles has been an extensively studied topic both theoretically[13–21] and experimentally.[7,8,22–24] Several experimental strategies involving benzo[*b*]- and benzo[*c*]- fused rings have been reported.[6–8] While benzo-annelated rings show more facile cycloaddition reactions, we thought it would be interesting to explore the cycloaddition of cyclobutano- and cyclobuteno-fused rings. This present study was expected to show the dependence on the nature of the fused rings of the reactivity of the diene and to assess how the product stability affects the activation energy. The present study concentrates on the more symmetrical [*c*]-fused rings which are expected to have a synchronous concerted mechanism in cycloaddition reactions with symmetrical dienophiles. Schleyer and coworkers reported that benzo[*c*]-fused dienes are more aromatic compared to their [*b*]-fused analogues based on NICS calculations.[25] The reactions between various dienophiles and anthracene, which may be considered as a benzo-annelated diene, are well known in the literature.[2b,20,26,27] Benzo-fused thiophenes are known for their applications in the pharmaceutical industry.[8c] The Diels–Alder strategy has been used in innovative ways to construct novel polycyclic cages using furan and its derivatives as dienes.[8] Jursic has studied the Diels–Alder reactivity of benzo[*b*]- and benzo[*c*]-fused thiophene, furan and pyrrole as dienes with various dienophiles at semiempirical levels of theory.[28] Manoharan *et al.* have studied the Diels–Alder reactions of benzo[*c*]-fused cyclopentadiene, furan and thiophene with ethylene as a dienophile.[20b] It is extremely important to obtain good estimates of the activation energy, reaction energy, *etc.* and computational chemistry provides a very promising and economical route to obtain these numbers and discern various effects, which ultimately help in designing the appropriate diene–dienophile combinations.

In the present study, we explore the cycloaddition reactions of cyclobutano[*c*]-, cyclobuteno[*c*]- and benzo[*c*]-fused cyclopentadiene, silole, pyrrole, phosphole, oxole and thiole with ethylene by various measures. These cycloaddition reactions are shown in Scheme 1. First, the geometries are discussed. A detailed analysis of the frontier orbitals and Fukui function indices at the reacting carbons of the dienes are discussed next. This is followed by the activation energies, reaction energies, thermochemical values and the distortion energies of the reactant pairs on going to the transition states.

Background of the computational methods

Modeling the Diels–Alder reactions has proved to be non-trivial and actually the inadequacies and inconsistencies of various theoretical methods have contributed significantly to controversy! Almost all the semiempirical methods show a consistent high preference for a stepwise over a concerted mechanism.[10,29] HF and CASSCF methods highly overestimate the barrier heights, while the MP2 methods underestimate it.

---

† Electronic supplementary information (ESI) available: figures and tables of the principal geometric parameters of all the dienes, transition states and products obtained at the B3LYP/6-31G* level and the Cartesian coordinates of all the optimized structures considered in this study. See http://www.rsc.org/suppdata/p2/b2/b205663a/

DOI: 10.1039/b205663a

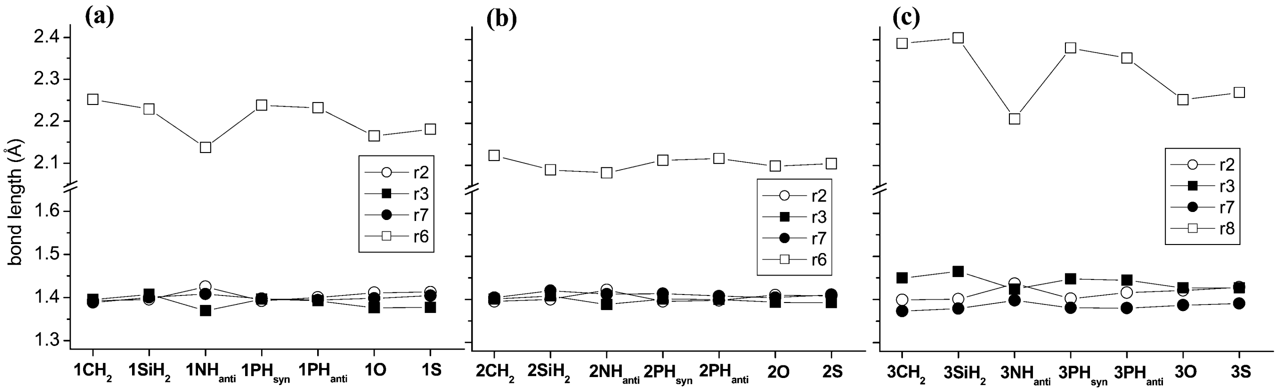

Fig. 1 Plot showing the important bond lengths (Å) obtained in the transition states of the cycloaddition reactions of dienes (a) **1**X; (b) **2**X and (c) **3**X with ethylene as the dienophile.

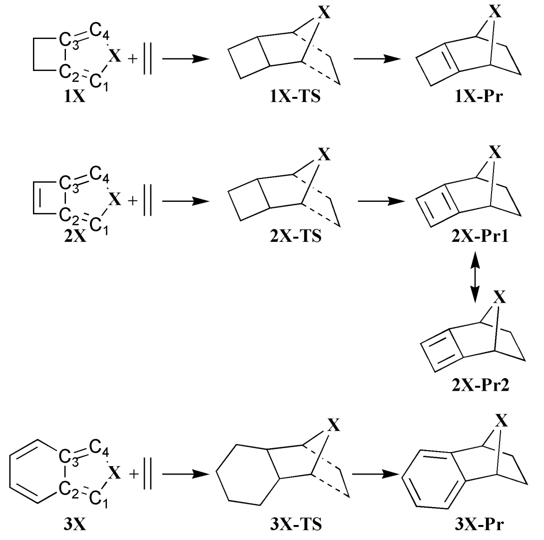

X = CH$_2$, SiH$_2$, NH, PH, O and S

Scheme 1

These results highlight the importance of including the dynamic electron correlation and simultaneously expose the inadequacy of MP2 formalism.[10,13a,30,31] Basis sets of double-ζ quality with a set of polarization functions, *e.g.*, 6-31G*, seem to be adequate. The hybrid density functional method, B3LYP was found to yield results in excellent agreement with the experimental results, especially regarding the barrier heights.[10,11,13,14] Among the conventional *ab initio* methods, one needs to employ CCSD(T) or at least MP3 to obtain quantitative results.[13a,16,17]

Computational details

All the dienes of planar form and ethylene were optimized at the B3LYP/6-31G* level. Frequency calculations were also done to characterize all the reactants. Except for **1**PH, **2**PH, **3**PH and **2**NH, all other planar dienes of C_{2v} point group are minima. Following the imaginary frequency for dienes **1**PH, **2**PH, **3**PH and **2**NH, the minimum energy structure for each of these dienes was obtained. The transition states and products for the Diels–Alder reactions of all the dienes considered were identified and optimized within the symmetry constraints at the same level of theory. Frequency calculations confirm the transition states and products by possessing one and zero imaginary frequencies, respectively. The B3LYP/6-31G* single point calculations for all the diene and dienophile components at the transition states were performed to calculate the distortion energies of dienes and dienophiles. All the calculations were done using the GAUSSIAN 98 suite of programs.[32] The normal modes of the transitions states were seen and confirmed as the cycloaddition transition states by using the MOPLOT program package.[33]

Results and discussion

Equilibrium geometries

The equilibrium geometries and the percentage stretching/shortening of the important bonds at the transition states are discussed in this section. The B3LYP/6-31G* optimized geometries for dienes **1**X, **2**X and **3**X are given in the supplementary material.† The designation for the geometric parameters of the transition states and products is depicted in Scheme 2. The optimized geometric parameters of all the transition states and products are given as supplementary material. In all the three types of diene, both *syn*- and *anti*-transition states and products were located for the PH substituted dienes. All efforts to locate *syn* transition states were futile for the NH substituted dienes, and only *anti*-transition states resulted. Nonetheless, both *syn*- and *anti*-products could be located as minima on the potential energy surfaces. The *syn*-transition state or product refers to the NH or PH bond located towards the diene side, whereas in the *anti* form, the NH or PH bond is placed towards the side of the incoming dienophile. The NH or PH bond lies in the bisector plane of the molecule in both *syn*- and *anti*-forms. The important bond lengths obtained for the transition states of all the three classes of diene are depicted in Fig. 1. The transition

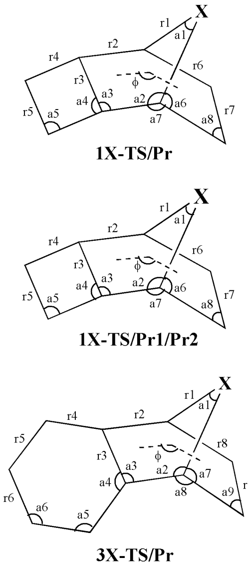

X = CH$_2$, SiH$_2$, NH, PH, O and S

Scheme 2

Table 1 The percentage stretching and shortening of the important bonds in the transition state for the reactions of dienes **1**X, **2**X and **3**X with ethylene, obtained at the B3LYP/6-31G* level

	%Stretching at the TS		%Shortening at the TS
	*r*2	*r*7	*r*3
1CH$_2$	28.0	24.5	49.5
1SiH$_2$	31.5	28.9	49.0
1NH[a]	37.2	33.5	55.6
1PH[b]	27.2 (31.9)	28.1 (27.0)	47.7 (50.9)
1O	34.4	29.3	54.2
1S	34.4	31.5	51.2
2CH$_2$	33.5	32.6	60.8
2SiH$_2$	37.4	38.7	64.1
2NH[a]	44.6	36.7	60.9
2PH[b]	34.4 (36.0)	36.1 (34.4)	60.8 (61.2)
2O	40.1	33.0	58.1
2S	39.6	35.7	58.5
3CH$_2$	23.7	18.1	45.3
3SiH$_2$	25.0	20.3	47.8
3NH[a]	35.3	29.1	59.6
3PH[b]	20.0 (29.6)	21.5 (21.3)	45.6 (50.0)
3O	31.3	24.5	54.9
3S	33.3	26.1	59.6

[a] Calculated for the *anti* form. [b] The values given in parentheses are for the *anti* form.

states of NH substituted dienes are the tightest in all the three classes of diene. However, the transition states possessing CH$_2$ substitution are the loosest in dienes **1**X and **2**X. The transition state of **3**SiH$_2$ is the loosest in the class of dienes **3**X. The transition states obtained for dienes **3**X are looser compared to dienes **1**X and **2**X. The transition states of Diels–Alder and other pericyclic reactions are aromatic due to the existence of cyclic π-electron delocalization.[34] The bond lengths *r*2, *r*3 and *r*7 are involved in delocalization in the transition states of all the three classes of diene. Fig. 1a indicates that the the transition states **1**CH$_2$-TS, **1**SiH$_2$-TS and both *syn*- and *anti*-**1**PH-TS are more aromatic in nature compared to *anti*-**1**NH-TS, **1**O-TS and **1**S-TS. Thus, the diene with the more aromatic five-membered ring experiences lower transition state stabilization.

Two products were obtained for the Diels–Alder reactions of dienes **2**X with ethylene and, in principle, two different transition states should be possible. Both the products (**2**X-Pr1 and **2**X-Pr2) possess an antiaromatic cyclobutadiene moiety as one of the rings. In the class of dienes **2**X, the transition state obtained corresponds to a [4 + 2] cycloaddition and results in **2**X-Pr1. However, the pseudoautomerization of the cyclobutadiene moiety results in **2**X-Pr2, which is of almost equal stability compared to **2**X-Pr1. Several attempts were made to obtain the transition state directly connecting **2**X and **2**X-Pr2, but all the attempts were futile and led only to **2**X-TS. Related situations were observed in electron transfer and polar transition states, which share and compete along the same reaction coordinate. In such cases, the mechanisms were entangled and only one transition state could be located as a stationary point on the potential energy surface.[35] In contrast to **1**X and **2**X systems, the **3**X system shows remarkable variations in the bond lengths in the benzenoid ring from reactant diene to product (see the supplementary material). This indicates that the reactions of dienes **3**X with ethylene follow [8 + 2] cycloaddition rather than [4 + 2] cycloaddition. The aromatic stabilized products *i.e.*, benzo-annelated norbornene and 7-substituted norbornene products are obtained. The percentage stretching/shortening of the particular bond at the transition state or product is obtained by calculating the ratio between the change in bond length of the particular bond from the reactant to the transition state and the same from the reactant to the product. Using the B3LYP/6-31G* bond lengths, the percentage stretching/shortening of the important bonds at the transition states were calculated and are presented in Table 1. The nature of the transition state as 'early' or 'late' is predicted using these percentage stretching/shortening values. The dienes with X = NH, O and S form late transition states whereas X = CH$_2$, SiH$_2$ and PH form early transition states for the classes of diene **1**X and **3**X. The transition states of dienes **2**X are late compared to the transition states of dienes **1**X and **3**X. In the classes of diene **1**X and **3**X, the aromatic dienes form tighter and late transition states compared to antiaromatic dienes.

Fukui function indices and FMO analysis

Local softness is used as a reactivity parameter to study the reactivity at any particular site of a chemical species.[36] The local softness, $s(\bar{r}) = f(\bar{r})S$, where $f(\bar{r})$ is the Fukui function introduced by Parr and Yang,[37] and S is the global softness.

Within Koopman's approximation, $S = 1/(\mathrm{IP} - \mathrm{EA})$, where IP and EA are taken as the negative of the HOMO and LUMO energies of the chemical species, respectively. Since both $s(\bar{r})$ and $f(\bar{r})$ contain the same information, the local softness values are given in this study. The local softness for any particular atom can be measured using eqns. (1) and (2),

$$s_k^+ = [\rho_k(N_0 + 1) - \rho_k(N_0)]S \qquad (1)$$

$$s_k^- = [\rho_k(N_0) - \rho_k(N_0 - 1)]S \qquad (2)$$

where $\rho_k(N_0)$, $\rho_k(N_0 - 1)$ and $\rho_k(N_0 + 1)$ are the electronic population on the atom k for the N_0, $N_0 - 1$ and $N_0 + 1$ electron system, respectively; these values were calculated using the Mulliken population analysis. At the UB3LYP/6-31G* level only the vertical states of anions and cations were considered. The values of s_k^+ and s_k^- are calculated for the reactive site (C$_1$ or C$_4$) for all the dienes and are given in Table 2 along with the HOMO–LUMO and LUMO–HOMO energy gaps between the diene and ethylene, and the extent of charge transfer from diene to dienophile at the transition state (q_{CT}). For all other dienes except **1**NH, **1**S, **2**NH, **2**PH, **2**O and **2**S, s_k^- values are higher than s_k^+ values. The dienes **1**S, **2**S and **3**S have the lowest softness values and are predicted to be the least reactive in their series. Normal electron demand, E_{N} is the flow of electron from diene to dienophile and from the dienophile to diene is known as inverse electron demand, E_{I}. In all the three types of diene, **1**X–**3**X, the dienes with X = CH$_2$, NH, O and S follow the normal electron demand except for the diene **2**CH$_2$, and X = SiH$_2$ and PH follow inverse electron demand. Except for the three dienes **1**PH, **2**CH$_2$ and **3**S, for all other dienes the extent of charge transfer from diene to dienophile at the transition state (q_{CT}) is in agreement with type of electron demand. The difference between the normal and inverse electron demand for the diene **3**S is much less, *i.e.*, 0.01 and the q_{CT} value is 0.001 at the B3LYP/6-31G* level, which makes the reaction of **3**S with ethylene a borderline case.

Energetics

Activation and reaction energies and thermochemical data. The activation energy, enthalpy, entropy and Gibbs free energies of activation for the cycloaddition reactions of dienes **1**X, **2**X and **3**X with ethylene at the B3LYP/6-31G* level are presented in Table 3. In general, the activation energies for the reactions of dienes **3**X with ethylene are lower compared to dienes of **1**X and **2**X types, and the trend predicted for the reactions of dienes **3**X is analogous to those of **1**X type. Lower activation energies in the reactions of dienes **3**X can be traced directly to the product stability, where an aromatic ring is generated in the product formed. In contrast, the products formed for dienes **2**X witness the formation of an antiaromatic ring in the product. Expectedly, the activation energies are highest in

Table 2 The frontier molecular orbital energies (E_{HOMO}, E_{LUMO}, in eV) of the dienes **1X**, **2X** and **3X**, the FMO energy gap between the diene and ethylene (E_N, E_I, in eV), the extent of charge transfer from the diene to dienophile in the transition state (q_{CT}) for all the reactions, and the local softness, s_k^+ and s_k^- values (in atomic units) for the reactive site (C_1 or C_4) for all the dienes considered in this study are given. The values were obtained at the B3LYP/6-31G* level

	E_{HOMO}	E_{LUMO}	E_N [a]	E_I [b]	q_{CT}	S_k^+	S_k^-
1CH_2	−5.56	−0.26	6.07	7.00	0.044	0.5368	0.7038
1SiH_2	−6.06	−1.21	6.57	6.05	−0.001	0.3837	0.7004
1NH	−5.38	1.17	5.89	8.43	0.111	0.5115	0.2431
1PH	−6.07	−0.93	6.59	6.33	0.000 (0.019) [c]	0.3719	0.6448
1O	−5.91	0.44	6.42	7.69	0.063	0.5863	0.7563
1S	−6.19	−0.25	6.70	7.01	0.015	0.3733	−0.0163
2CH_2	−6.00	−0.95	6.51	6.30	0.031	0.4464	0.4762
2SiH_2	−6.52	−1.27	7.03	5.98	−0.006	0.3424	0.3866
2NH	−4.90	−0.67	5.41	6.58	0.084	0.5993	0.4349
2PH	−5.83	−1.25	6.34	6.01	−0.010 (0.006) [c]	0.3858	0.1884
2O	−5.58	−1.08	6.09	6.18	0.040	0.6265	0.4810
2S	−5.38	−1.18	5.89	6.08	−0.007	0.4080	0.0858
3CH_2	−4.92	−1.59	5.43	5.67	0.022	0.5997	0.8612
3SiH_2	−5.25	−2.30	5.76	4.96	−0.029	0.4727	0.8718
3NH	−4.79	−0.40	5.31	6.85	0.092	0.4963	0.8192
3PH	−5.26	−1.97	5.78	5.29	−0.019 (0.001) [c]	0.4242	0.7136
3O	−5.25	−1.11	5.77	6.14	0.043	0.6014	0.8744
3S	−5.37	−1.36	5.88	5.89	0.001	0.3536	0.6040

[a] $E_N = E_{HOMO}$(diene) – 0.51 eV [E_{LUMO}(ethylene)]. [b] $E_I = E_{LUMO}$ (diene) – (−7.26 eV) [E_{HOMO} (ethylene)]. [c] The extent of charge transfer from diene to dienophile (q_{CT}) at the *anti* transition state.

Table 3 The activation energy ($\Delta E^\ddagger$), enthalpy ($\Delta H^\ddagger$), entropy ($\Delta S^\ddagger$) and Gibbs free energy ($\Delta G^\ddagger$) of activation for the cycloaddition reactions of dienes **1X**, **2X** and **3X** with ethylene obtained at the B3LYP/6-31G* level. All the values are given in kcal mol^{-1}

		$\Delta E^\ddagger$	$\Delta H^\ddagger$	$\Delta S^\ddagger$	$\Delta G^\ddagger$
1CH_2		19.7	20.9	−12.1	33.0
1SiH_2		21.4	22.4	−12.3	34.7
1NH	*anti*	28.3	29.3	−12.4	41.7
1PH	*syn*	24.8	25.8	−12.5	38.3
	anti	25.4	26.4	−12.6	39.0
1O		23.3	24.1	−12.1	36.2
1S		33.2	34.0	−12.1	46.1
2CH_2		35.5	36.3	−12.0	48.3
2SiH_2		42.0	42.5	−12.0	54.5
2NH	*anti*	35.0	35.9	−12.7	48.6
2PH	*syn*	39.6	40.3	−12.3	52.6
	anti	41.0	41.7	−12.5	54.2
2O		31.6	32.3	−12.1	44.4
2S		41.7	42.2	−12.0	54.2
3CH_2		10.8	11.9	−11.9	23.8
3SiH_2		9.8	10.6	−12.0	22.6
3NH	*anti*	21.4	22.4	−12.1	34.5
3PH	*syn*	16.4	17.2	−12.3	29.5
	anti	15.2	16.2	−12.5	28.7
3O		15.4	16.2	−12.0	28.2
3S		24.7	25.5	−12.0	37.5

this class of reaction. Hence the products of **2X** are expected to undergo retro-Diels–Alder reactions to form dienes **2X** and ethylene. Thus, in practice, while the **1X** and **3X** series represent Diels–Alder reactions, for the **2X** series it may be appropriate to categorize it as retro-Diels–Alder type. At the same level of theory, the reaction energies, reaction enthalpies, reaction entropies and Gibbs free energies of reactions of dienes **1X**, **2X** and **3X** with ethylene as dienophile are given in Table 4. Due to the presence of lone pair electrons on the heteroatoms, the dienes **1**NH, **1**PH, **1**O and **1**S have the cyclic 6π-electron delocalization, hence the five-membered rings of these dienes are considered to be aromatic. To our knowledge the aromaticity ordering for dienes **1**NH, **1**PH, **1**O and **1**S has not yet been determined. Schleyer *et al.* predicted the aromaticity ordering for the five-membered ring dienes, and the aromaticity decreases in the following order: pyrrole > thiophene > furan > phosphole.[38] The relationship between the aromaticity of the diene and the activation barrier of Diels–Alder reactions has been fairly well established.[13,18h,20b,28] Thus, the feasibility of the reaction is higher with a less aromatic diene. Due to the aromatic nature of dienes **1**NH, **1**PH, **1**O and **1**S in the class of dienes **1X**, one may expect a similar trend in activation and reaction energies as we obtained for the reactions of monocyclic five-membered ring dienes with ethylene reported in our recent study.[13a] Table 3 shows that the reactivity of dienes **1X** based on activation energy decreases in the following order: **1**CH_2, **1**SiH_2, **1**O, **1**PH, **1**NH and **1**S. The reaction energy data given in Table 4 indicate that the exothermicity for the reactions of dienes **1X** with ethylene decreases in the following order of dienes: **1**CH_2, **1**SiH_2, **1**PH, **1**O, **1**S and **1**NH. The reactivity ordering based on the activation energies is not analogous but the exothermicity order is very similar to our earlier study involving monocyclic five-membered ring dienes with ethylene as dienophile at the B3LYP/6-31G* level.[13a]

Similar to dienes **1**NH, **1**PH, **1**O and **1**S, the dienes **3**NH, **3**PH, **3**O and **3**S are aromatic, where 10π-electrons are involved in delocalization. The activation and reaction energies given in Tables 3 and 4, respectively, show that the reactivity ordering based on the activation energies and the exothermicity ordering of dienes **3X** is similar to that of dienes **1X** except for **3**SiH_2 and **3**CH_2. Here the diene **3**SiH_2 is predicted to be more reactive and 0.5 kcal mol^{-1} more exothermic than **3**CH_2. In **1X** and **3X**, the dienes possessing an aromatic five-membered ring are predicted to be less reactive and less exothermic compared to dienes containing an antiaromatic five-membered ring on reaction with ethylene as dienophile. This may be traced to the disruption of aromaticity in the five-membered rings.

Table 3 shows that the activation energy for dienes **2X** increases in the following order: **2**O, **2**NH, **2**CH_2, **2**PH, **2**S and **2**SiH_2. The reactivity of dienes **2**SiH_2 and **2**S are energetically competitive since the diene **2**SiH_2 requires only 0.3 kcal mol^{-1} more activation energy than for the diene **2**S. Similar to this situation, the diene **2**CH_2 requires only 0.5 kcal mol^{-1} higher activation energy than for the diene **2**NH. The reaction energies given in Table 4 show that the endothermicity increases in the following order of dienes for the formation of product **1** (**2X**-Pr1): **2**CH_2, **2**O, **2**PH, **2**NH, **2**S, **2**SiH_2. In this order, the diene **2**NH is considered for the formation of only the *anti*-product. This order is not retained in the formation of product **2** (**2X**-Pr2). Similar to product **1** (**2X**-Pr1), here also the formation of **2**CH_2-Pr2 is less endothermic and **2**SiH_2-Pr2 is more

Table 4 The reaction energy (ΔE_r), reaction enthalpy (ΔH_r), entropy (ΔS_r) and Gibbs free energy (ΔG_r) of reaction for the cycloaddition reactions of dienes **1**X, **2**X and **3**X with ethylene obtained at the B3LYP/6-31G* level. The values given in parentheses are for the product **2** (**2**X-Pr2). All the values are given in kcal mol^{-1}

		ΔE_r	ΔH_r	ΔS_r	ΔG_r
1CH$_2$		−23.2	−18.9	−13.2	−5.7
1SiH$_2$		−17.1	−13.3	−13.1	−0.3
1NH	*syn*	−4.0	−0.3	−13.3	13.0
	anti	−0.3	3.1	−13.2	16.3
1PH	*syn*	−15.0	−11.0	−13.6	2.6
	anti	−16.8	−12.8	−13.5	0.7
1O		−10.8	−7.4	−12.9	5.5
1S		−4.8	−1.2	−12.9	11.7
2CH$_2$		3.3 (6.8)	6.7 (10.1)	−13.0 (−12.8)	19.7 (22.9)
2SiH$_2$		17.1 (16.9)	19.8 (19.6)	−12.8 (−12.7)	32.6 (32.3)
2NH	*syn*	7.6 (11.2)	11.0 (14.4)	−13.5 (−13.3)	24.5 (27.7)
	anti	11.9 (16.1)	15.1 (18.9)	−13.6 (−13.3)	28.7 (32.2)
2PH	*syn*	10.6 (7.8)	13.7 (11.0)	−13.5 (−13.3)	27.2 (24.3)
	anti	10.3 (10.9)	13.5 (14.0)	−13.4 (−13.2)	26.9 (27.2)
2O		4.4 (8.6)	7.5 (11.4)	−13.0 (−12.6)	20.5 (24.0)
2S		12.2 (9.7)	15.3 (12.7)	−13.0 (−12.7)	28.3 (25.4)
3CH$_2$		−48.8	−44.0	−13.5	−30.5
3SiH$_2$		−49.3	−45.1	−13.5	−31.6
3NH	*syn*	−18.2	−14.4	−13.2	−1.2
	anti	−16.2	−12.5	−13.2	0.7
3PH	*syn*	−43.0	−38.6	−13.8	−24.8
	anti	−43.7	−39.3	−13.8	−25.5
3O		−29.8	−26.0	−13.1	−12.9
3S		−27.1	−23.1	−13.1	−10.0

endothermic than the others. Calculations predict that the Diels–Alder reactions of dienes **2**X type with ethylene require a high activation energy and are highly endothermic compared to dienes **1**X and **3**X.

Good linear correlation is observed between the activation energies and reaction energies for all the dienes considered in this study, and is shown in Fig. 2. In this plot, the activation energies for all the available transition states and the reaction energies of products corresponding to the transition states are considered. The *anti*-1PH-TS and *anti*-2PH-TS lie respectively 0.6 and 1.4 kcal mol^{-1} above their corresponding *syn*-transition states on their respective potential energy surfaces, whereas the diene **3**PH requires 1.2 kcal mol^{-1} less activation energy to form the *anti*-3PH-TS compared to *syn*-3PH-TS. The *anti*-products of all the PH substituted dienes are more exothermic than *syn*-products except for *anti*-2PH-Pr2. In contrast to the PH substituted dienes, the reactions of NH substituted dienes with ethylene to form *anti*-products are less exothermic compared to those forming *syn*-products. The difference in energy between *syn*- and *anti*-products obtained for diene **1**NH is 3.7 kcal mol^{-1} and for **3**NH is only 2.0 kcal mol^{-1}. In case of diene **2**NH, this difference is 4.3 and 4.9 kcal mol^{-1}, respectively, for **2**NH-Pr1 and **2**NH-Pr2.

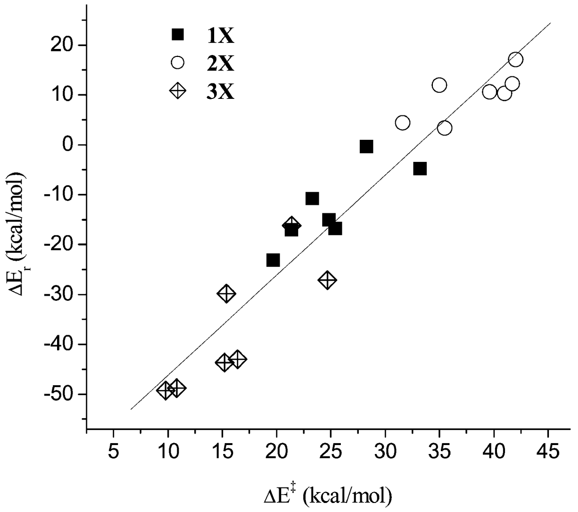

Fig. 2 Plot showing the correlation of activation energy *versus* reaction energy for the cycloaddition reactions of all three classes of diene **1**X–**3**X with ethylene as the dienophile.

The entropy of activation values given in Table 3 become less negative or almost the same for all the dienes on going from **1**X to **2**X then to **3**X. There is no steady change in reaction entropy values on going from **1**X to **2**X, whereas the values become more negative on going either from **1**X to **3**X or from **2**X to **3**X for most of the dienes, and this is clearly seen from Table 4.

Distortion energies

Calculation of the energy difference between the reactants in the transition state geometry and their equilibrium geometries will indicate how much both the diene and dienophile are distorted to reach the transition state structure. The total distortion energy is the sum of the distortion energies of the diene and dienophile. The distortion energies of diene and dienophile, and the total distortion energies along with the interaction and activation energies at the B3LYP/6-31G* level are given in Table 5. The interaction energy is obtained by subtracting the total distortion energy from the activation energy. The total distortion energy values of dienes **1**X are in between those of dienes **2**X and **3**X. Thus, the distortion energies explain why the reactions of dienes **3**X with ethylene require less activation energy and the dienes **2**X require very high activation energy in these three classes of diene. Table 5 shows that the dienes and ethylene are much distorted at **2**X-TS, whereas their distortion is very much less at **3**X-TS compared to the others. The reaction in which the diene or ethylene is very much distorted at the transition state, has a higher activation energy compared to other reactions in all three classes. The total distortion energy and also the distortion energy of ethylene are maximum for **1**NH-TS, **2**SiH$_2$-TS and **3**NH-TS in the dienes **1**X, **2**X and **3**X, respectively. The highest interaction energy is observed for the NH substituted dienes uniformly in all the three classes of diene. Comparison of Tables 4 and 5 indicates that, in general, the diene which has lower total distortion energy yields a more exothermic product and *vice-versa*. The total and reactant distortion energies are lower at the *anti* transition state compared to *syn* transition state for all the PH substituted dienes.

Table 5 The distortion energies of the dienes and ethylene, the total distortion energy, the interaction energy and the activation energy ($\Delta E^{\ddagger}$) for cycloaddition reactions of dienes **1**X, **2**X and **3**X with ethylene. The values are obtained at the B3LYP/6-31G* level. All the values are given in kcal mol^{-1}

	Distortion energy			Interaction energy	$\Delta E^{\ddagger}$
	Diene	Ethylene	Total		
1CH_2	16.4	7.7	24.1	−4.4	19.7
1SiH_2	16.3	10.4	26.7	−5.4	21.4
1NH[a]	23.4	13.4	36.8	−8.5	28.3
1PH[b]	20.9 (18.4)	9.5 (9.4)	30.4 (27.9)	−5.6 (−2.5)	24.8 (25.4)
1O	19.7	10.4	30.1	−6.8	23.3
1S	24.8	11.6	36.4	−3.2	33.2
2CH_2	26.5	11.8	38.3	−2.8	35.5
2SiH_2	28.9	16.2	45.1	−3.1	42.0
2NH[a]	28.3	14.5	42.8	−7.8	35.0
2PH[b]	29.5 (29.4)	13.9 (13.3)	43.4 (42.7)	−3.8 (−1.7)	39.6 (41.0)
2O	25.6	12.1	37.7	−6.1	31.6
2S	31.0	13.7	44.7	−3.0	41.7
3CH_2	10.3	4.1	14.4	−3.5	10.9
3SiH_2	8.9	4.9	13.8	−4.0	9.8
3NH[a]	19.1	10.1	29.2	−7.8	21.4
3PH[b]	15.6 (11.5)	5.2 (5.5)	20.8 (17.0)	−4.4 (−1.8)	16.4 (15.2)
3O	14.5	7.1	21.6	−6.2	15.4
3S	19.3	8.1	27.4	−2.7	24.7

[a] The values are given for the *anti* transition states. [b] The values given in parentheses are for the *anti* transition states.

Conclusions

The present study reports a computational study of the cycloaddition reactions of [*c*]-annelated five-membered carbo- and hetero-cyclic dienes with ethylene. Among the three classes of diene, the class **3**X requires lower activation energies and the products formed are more exothermic on reaction with ethylene as dienophile. Next, lower activation energies are required for the reactions of dienes **1**X with ethylene, and the products formed are less exothermic compared to **3**X-Pr. The class of dienes **2**X requires much higher activation energies compared to other classes of diene, and all the reactions for the formation of both the types of product, **2**X-Pr1 and **2**X-Pr2 are more endothermic. Therefore, the current results indicate that Diels–Alder reactions of dienes **2**X with ethylene are not viable and the products of **2**X, the cyclobuteno-annelated norbornene and 7-heteronorbornene, are expected to participate in retro-Diels–Alder reactions. An examination of the geometries indicates that, while all the reactions involving **1**X and **2**X type dienes conform to [4 + 2] cycloaddition, those involving benzo[*c*]-annelated dienes may be treated as [8 + 2] cycloadditions. Analysis of the percentage stretching/shortening of the important bonds in the transition state reveals that the aromatic dienes form late and tight transition states compared to non-aromatic or antiaromatic dienes. The transition states formed are late for the reactions of dienes **2**X with ethylene. FMO analysis predicts that the reactions of dienes with X = SiH_2 and PH in all three classes of diene **1**X–**3**X are of inverse electron demand type, and all other dienes except **2**CH_2 follow normal electron demand. The extent of charge transfer at the transition state (q_{CT}) is in agreement with electronic demand for the reactions of most of the dienes with ethylene. Good correlation between the activation and reaction energies is seen for all the dienes. The diene requiring the maximum activation energy is predicted to have either a highly distorted diene or dienophile geometry at the transition state. Aromatic dienes have higher distortion energies than antiaromatic dienes in **1**X and **3**X, which is in agreement with the activation and reaction energies. Among the three classes of diene, the distortion energies are lower for **3**X and higher for dienes of type **2**X. [*b*]-Fused heterocyclic dienes are also important synthetic precursors for novel polycyclic frameworks. Studies on this class of compound are currently in progress and will be reported separately.

Acknowledgements

Recognition and support by UGC, New Delhi in the form of the SAP-DRS scheme and DST-FIST to the Department of Chemistry, Pondicherry University are gratefully acknowledged. T. C. D. thanks CSIR, New Delhi for a research fellowship. R. Vijaya is thanked for doing some preliminary calculations.

References

1 (*a*) R. B. Woodward and R. Hoffmann, *Angew. Chem., Int. Ed. Engl.*, 1969, **8**, 781; (*b*) I. Fleming, *Frontier Orbitals and Organic Chemical Reactions*, Wiley, Chichester, 1976.

2 (*a*) K. N. Houk, Y. Li and J. D. Evanseck, *Angew. Chem., Int. Ed. Engl.*, 1992, **31**, 682; (*b*) J. Sauer and R. Sustmann, *Angew. Chem., Int. Ed. Engl.*, 1980, **19**, 779.

3 (*a*) W. Carruthers, *Cycloaddition Reactions in Organic Synthesis; Tetrahedron Organic Chemistry Series*, Pergamon, Elmsford, NY, 1990; (*b*) D. L. Boger, *Chem. Rev.*, 1986, **86**, 781.

4 (*a*) S. Kuroda, M. Oda, S. Zuo, K. Kanayama, S. I. M. Shah, S. Furuta, R. Miyataka and M. Kyogoku, *Tetrahedron Lett.*, 2001, **42**, 6345; (*b*) P. R. Carly, S. L. Cappelle, F. Compernolle and G. J. Hoornaert, *Tetrahedron*, 1996, **52**, 11889; (*c*) J. L. Charlton and M. M. Alauddin, *Tetrahedron*, 1987, **43**, 2873; (*d*) M. Haber and U. Pindur, *Tetrahedron*, 1991, **47**, 1925.

5 (*a*) R. P. Thummel, W. E. Cravey and W. Nutakul, *J. Org. Chem.*, 1978, **43**, 2473; (*b*) R. P. Thummel and W. Nutakul, *J. Am Chem. Soc.*, 1978, **100**, 6171.

6 S. V. D. Andrea, J. P. Freeman and J. Szmuszkovicz, *J. Org. Chem.*, 1990, **55**, 4356.

7 Z. Chen and M. L. Trudell, *Chem. Rev.*, 1996, **96**, 1179.

8 (*a*) P. Vogel, J. Cossy, J. Plumet and O. Arjona, *Tetrahedron*, 1999, **55**, 13521; (*b*) J. D. Winkler, *Chem. Rev.*, 1996, **95**, 167; (*c*) C. W. Bird, in *Comprehensive Heterocyclic Chemistry II*, eds. A. R. Katritzky, C. W. Rees and E. F. V. Scriven, vol. 2, Pergamon Press, Elsevier Science Ltd, Oxford, UK, 1996.

9 K. N. Houk, J. Gonzalez and Y. Li, *Acc. Chem. Res.*, 1995, **28**, 81.

10 E. Goldstein, B. Beno and K. N. Houk, *J. Am. Chem. Soc.*, 1996, **118**, 6036.

11 B. R. Beno, S. Wilsey and K. N. Houk, *J. Am. Chem. Soc.*, 1999, **121**, 4816.

12 S. Sakai, *J. Phys. Chem. A*, 2000, **104**, 922.

13 (*a*) T. C. Dinadayalane, R. Vijaya, A. Smitha and G. N. Sastry, *J. Phys. Chem. A*, 2002, **106**, 1627; (*b*) R. Vijaya, T. C. Dinadayalane and G. N. Sastry, *J. Mol. Struct. (Theochem)*, 2002, **589–590**, 303.

14 K. N. Houk, B. R. Beno, M. Nendel, K. Black, H. Y. Yoo, S. Wilsey and J. K. Lee, *J. Mol. Struct. (Theochem)*, 1997, **398–399**, 169.

15 K. N. Houk, R. J. Loncharich, J. F. Blake and W. L. Jorgensen, *J. Am. Chem. Soc.*, 1989, **111**, 9172.

16 W. L. Jorgensen, D. Lim and J. F. Blake, *J. Am. Chem. Soc.*, 1993, **115**, 2936.

17 S. M. Bachrach and M. Liu, *J. Org. Chem.*, 1992, **57**, 6736.

18 (*a*) B. S. Jursic, Z. Zdravkovski and S. L. Whittenburg, *J. Chem. Soc., Perkin Trans. 2*, 1996, 455; (*b*) B. S. Jursic and Z. Zdravkovski, *J. Mol. Struct. (Theochem)*, 1995, **332**, 39; (*c*) B. S. Jursic, *J. Chem. Soc., Perkin Trans. 2*, 1999, 373; (*d*) B. S. Jursic and Z. Zdravkovski, *J. Org. Chem.*, 1995, **60**, 2865; (*e*) B. S. Jursic and Z. Zdravkovski, *J. Mol. Struct. (Theochem)*, 1995, **331**, 215; (*f*) B. S. Jursic, *Tetrahedron Lett.*, 1997, **38**, 1423; (*g*) B. S. Jursic and Z. Zdravkovski, *J. Chem. Soc., Perkin Trans. 2*, 1995, 1223; (*h*) B. S. Jursic, *J. Mol. Struct. (Theochem)*, 1998, **454**, 105.

19 M. Manoharan and P. Venuvanalingam, *J. Chem. Soc., Perkin Trans. 2*, 1996, 1423.

20 (*a*) M. Manoharan and P. Venuvanalingam, *Int. J. Quantum Chem.*, 1998, **66**, 309; (*b*) M. Manoharan, F. De Proft and P. Geerlings, *J. Chem. Soc., Perkin Trans. 2*, 2000, 1767.

21 S. Calvo-Losada and D. Suarez, *J. Am. Chem. Soc.*, 2000, **122**, 390.

22 (*a*) M. Avalos, R. Babiano, J. L. Bravo, P. Cintas, J. L. Jimenez, J. C. Palacios and M. A. Silva, *J. Org. Chem.*, 2000, **65**, 6613; (*b*) M. J. S. Dewar and A. B. Pierini, *J. Am. Chem. Soc.*, 1984, **106**, 203; (*c*) Y. Li, T. Thiemann, T. Sawada, S. Mataka and M. Tashiro, *J. Org. Chem.*, 1997, **62**, 7926.

23 P. L. Goff, F. Mathey and L. Ricard, *J. Org. Chem.*, 1989, **54**, 4754.

24 (*a*) R. Walsh and J. M. Wells, *J. Chem. Soc., Perkin Trans. 2*, 1975, 52; (*b*) B. A. Horn, J. L. Herek and A. H. Zewail, *J. Am. Chem. Soc.*, 1996, **118**, 8755; (*c*) A. H. Zewail, *J. Phys. Chem.*, 1996, **100**, 12701.

25 G. Subramanian, P. v. R. Schleyer and H. Jiao, *Angew. Chem., Int. Ed. Engl.*, 1996, **35**, 2638.

26 (*a*) Y. Chung, B. F. Duerr, T. A. Mckelvey, P. Nanjappan and A. W. Czarnik, *J. Org. Chem.*, 1989, **54**, 1018; (*b*) V. D. Kiselev, E. A. Kashaeva and A. I. Konovalov, *Tetrahedron*, 1999, **55**, 1153.

27 M. Manoharan and P. Venuvanalingam, *J. Phys. Org. Chem.*, 1998, **11**, 133.

28 (*a*) B. S. Jursic, *Tetrahedron*, 1997, **53**, 13285; (*b*) B. S. Jursic, *J. Chem. Soc., Perkin Trans. 2*, 1995, 1217.

29 (*a*) K. N. Houk, Y. -T. Lin and F. K. Brown, *J. Am. Chem. Soc.*, 1986, **108**, 554; (*b*) F. K. Brown and K. N. Houk, *Tetrahedron Lett.*, 1984, **25**, 4609; (*c*) M. J. S. Dewar, S. Olivella and J. J. P. Stewart, *J. Am. Chem. Soc.*, 1986, **108**, 5771.

30 B. S. Jursic, *J. Org. Chem.*, 1997, **62**, 3046.

31 (*a*) Y. Li and K. N. Houk, *J. Am. Chem. Soc.*, 1993, **115**, 7478; (*b*) R. D. J. Froese, J. M. Coxon, S. C. West and K. Morokuma, *J. Org. Chem.*, 1997, **62**, 7971; (*c*) M. Manoharan, F. De Proft and P. Geerlings, *J. Org. Chem.*, 2000, **65**, 7971.

32 GAUSSIAN 98, Revision A.11.2, M. J. Frisch, G. W. Trucks, H. B. Schlegel, G. E. Scuseria, M. A. Robb, J. R. Cheeseman, V. G. Zakrzewski, J. A. Montgomery Jr., R. E. Stratmann, J. C. Burant, S. Dapprich, J. M. Millam, A. D. Daniels, K. N. Kudin, M. C. Strain, O. Farkas, J. Tomasi, V. Barone, M. Cossi, R. Cammi, B. Mennucci, C. Pomelli, C. Adamo, S. Clifford, J. Ochterski, G. A. Petersson, P. Y. Ayala, Q. Cui, K. Morokuma, N. Rega, P. Salvador, J. J. Dannenberg, D. K. Malick, A. D. Rabuck, K. Raghavachari, J. B. Foresman, J. Cioslowski, J. V. Ortiz, A. G. Baboul, B. B. Stefanov, G. Liu, A. Liashenko, P. Piskorz, I. Komaromi, R. Gomperts, R. L. Martin, D. J. Fox, T. Keith, M. A. Al-Laham, C. Y. Peng, A. Nanayakkara, M. Challacombe, P. M. W. Gill, B. G. Johnson, W. Chen, M. W. Wong, J. L. Andres, C. Gonzalez, M. Head-Gordon, E. S. Replogle and J. A. Pople, GAUSSIAN, Inc., Pittsburgh PA, 2001.

33 T. Bally, B. Albrecht, S. Matzinger and G. M. Sastry, MOPLOT 3.2, University of Fribourg, 1997.

34 (*a*) M. G. Evans and E. Warhurst, *Trans. Faraday Soc.*, 1938, **34**, 614; (*b*) H. Zimmerman, *Acc. Chem. Res.*, 1971, **4**, 272.

35 (*a*) G. N. Sastry and S. Shaik, *J. Am. Chem. Soc.*, 1998, **120**, 2131; (*b*) A. C. Reddy, D. Danovich, A. Ioffe and S. Shaik, *J. Chem. Soc., Perkin Trans. 2*, 1995, 1525; (*c*) G. N. Sastry, A. C. Reddy and S. Shaik, *Angew. Chem., Int. Ed. Engl.*, 1995, **34**, 1495.

36 (*a*) R. G. Parr and W. Yang, *Density Functional Theory of Atoms and Molecules*, Oxford University Press, Oxford, 1989; (*b*) R. K. Roy, S. Pal and K. Hirao, *J. Chem. Phys.*, 1999, **110**, 8236.

37 R. G. Parr and W. Yang, *J. Am. Chem. Soc.*, 1984, **106**, 4049.

38 (*a*) P. v. R. Schleyer, P. K. Freeman, H. Jiao and B. Goldfuss, *Angew. Chem., Int. Ed. Engl.*, 1995, **34**, 337; (*b*) P. v. R. Schleyer, C. Maerker, A. Dransfeld, H. Jiao and N. J. R. van Eikema Hommes, *J. Am. Chem. Soc.*, 1996, **118**, 6317.